Journal of Hazardous Materials 461 (2024) 132564

Contents lists available at ScienceDirect

Journal of Hazardous Materials

journal homepage: www.elsevier.com/locate/jhazmat

Visible light-activated photosensitizer inhibits the plasmid-mediated horizontal gene transfer of antibiotic resistance genes

Yan-Zi Wang [a,b], Xin-Li An [a,b], Xiao-Ting Fan [a,b], Qiang Pu [c], Hu Li [a,b], Wen-Zhen Liu [b,d], Zhuo Chen [b,d], Jian-Qiang Su [a,b,*]

[a] Key Laboratory of Urban Environment and Health, Ningbo Observation and Research Station, Institute of Urban Environment, Chinese Academy of Sciences, 1799 Jimei Road, Xiamen 361021, China
[b] University of Chinese Academy of Sciences, 19A Yuquan Road, Beijing 100049, China
[c] State Key Laboratory of Environmental Geochemistry, Institute of Geochemistry, Chinese Academy of Sciences, Guiyang 550081, China
[d] State Key Laboratory of Structural Chemistry, CAS Key Laboratory of Design and Assembly of Functional Nanostructures, and Fujian Key Laboratory of Nanomaterials, Fujian Institute of Research on the Structure of Matter, Chinese Academy of Sciences, Fuzhou, Fujian 350002, China

HIGHLIGHTS

- VLRB inhibits the transformation and conjugation of plasmids.
- VLRB induces photodegradation of plasmids.
- VLRB regulates conjugation-related gene expression.
- VLRB has potential in the mitigation of plasmid-encoded ARG transfer.

GRAPHICAL ABSTRACT

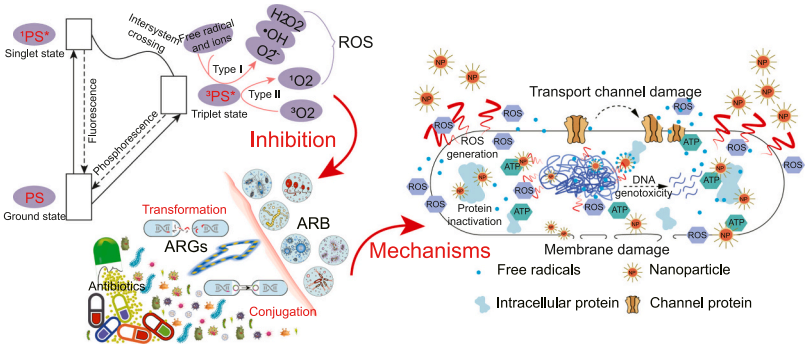

ARTICLE INFO

Editor: Karina Gin

Keywords:
Antibiotic resistance genes
Horizontal gene transfer
Transformation
Conjugation
Photosensitizer

ABSTRACT

Inhibition of plasmid transfer, including transformation and conjugation, is essential to prevent the spread of plasmid-encoded antimicrobial resistance. Photosensitizers have been successfully used in the treatment of serious infectious diseases, however, the effects of photosensitizers on the plasmid transfer are still elusive. In this study, we determined the transformation and conjugation efficiency of plasmid pUC19 and pRP4, respectively, when exposed to a photosensitizer (Visible Light-activated Rose Bengal, VLRB). The results showed that the activation of VLRB resulted in up to a 580-fold decrease in the transformation frequency of pUC19 and a 10-fold decrease in the conjugation frequency of pRP4 compared with the non-VLRB control. The inhibition of pUC19 transformation by VLRB exhibited a dose-dependent manner and was attributed to the changes in the plasmid conformation. The inhibition of pRP4 conjugation was associated with the generation of extracellular free radicals, induced oxidative stress, suppression of the mating pair formation gene (*trbBp*) and DNA transfer and replication gene (*trfAp*), and enhanced expression of the global regulatory genes (*korA*, *korB*, and *trbA*). These

* Corresponding author at: Key Laboratory of Urban Environment and Health, Ningbo Observation and Research Station, Institute of Urban Environment, Chinese Academy of Sciences, 1799 Jimei Road, Xiamen 361021, China.
E-mail address: jqsu@iue.ac.cn (J.-Q. Su).

https://doi.org/10.1016/j.jhazmat.2023.132564
Received 26 July 2023; Received in revised form 4 September 2023; Accepted 13 September 2023
Available online 16 September 2023

findings highlight the potential of visible light-activated photosensitizer for mitigating the dissemination of plasmid-encoded antibiotic resistance genes.

1. Introduction

The rapid emergence and spread of antibiotic resistance in pathogens are endangering the efficacy of antibiotics, significantly challenging the treatment of bacterial infections worldwide. Antibiotic resistance can be acquired by mutations or by horizontal gene transfer (HGT), which is the driving mechanism for the shuttling and spreading of antibiotic resistance genes (ARGs) among different microorganisms via mobile genetic elements (MGEs), exacerbating the pandemic and propagation of ARGs. The main mechanisms of HGT for ARGs include transformation (uptake of extracellular DNA), conjugation (mediated by integrative conjugative elements and plasmids), and transduction (mediated by bacteriophages) [1]. Studies have revealed that HGT events of ARGs are prevalent, and numerous contaminants, e.g., antibiotics, nanomaterials, heavy metals, and a wide range of chemicals, can significantly facilitate the horizontal transfer of ARGs in different ecological niches [2-6]. The development of methods to prevent HGT is pivotal for tackling the growing global threat of antibiotic resistance.

Several compounds are conjugation- or transformation-related inhibitors in vitro, e.g., relaxase inhibitors, pilus blockers, 2-Alkynoic fatty acids, and other nonspecific inhibitors [7,8]. These compounds can be employed to specifically target the plasmid horizontal transfer machinery including the cell membranes of both donor and recipient strains, the bacterial oxidative stress-response systems, the expression of transfer-related genes, and the nucleic acid (both the DNA structure and composition). The synthetic 2-alkynoic fatty acids were found to act on the donor cell, e.g., *Escherichia*, *Salmonella*, *Pseudomonas*, and *Acinetobacter* spp., inhibiting the transfer of lncW, linW, and lncH plasmids [8]. The synthetic fatty acid 2-hexadecynoic acid (2-HDA), having the ability to block the plasmid secretion machinery, when used as a food supplement in freshwater microcosms or mouse systems, the conjugation efficiency of model plasmids was reduced 10-fold or 50-fold, respectively [9]. However, the spectrum of synthetic compounds that blocks horizontal gene transfer to inhibit the spread of antibiotic resistance genes in the environment is still limited and their potential side effect remains undetermined. Still, there is a need for new agents which can efficiently counteract ARGs transfer.

Photosensitizers are a group of chemical agents including porphyrin, bacteriochlorin derivatives, and phthalocyanines, which can be excited to a long-lived triplet state, and react with molecular oxygen upon activation via light with specific wavelengths to generate reactive singlet oxygen [10]. The photodynamic process refers to the formation of free radicals by electron transfer reactions, followed by the production of reactive oxygen species (ROS) including the superoxide ions ($O_2^{\bullet-}$), hydroxyl radicals (•OH), and hydrogen peroxide (H_2O_2) in Type-I electron transfer reactions, and production of singlet oxygen ($^1O_2$) in Type-II reactions [11,12]. Based on their molecular photocatalytic properties, photosensitizers have been widely applied in the treatment of cancer and some other diseases [13-17]. Photosensitizers, light, and oxygen are three essential components of photodynamic therapy (PDT). Several recent studies have demonstrated that photosensitizers such as phenothiazines, acridines, phthalocyanines chlorins, and porphyrins can be used as an effective therapy to treat a broad spectrum of infectious microorganisms owing to their antimicrobial activities originating from cytotoxic ROS production [18-20]. The oxidative molecules can damage microbial macromolecules such as lipids, proteins, and nucleic acids, resulting in bacterial cell death [21]. Due to their major advantages of antimicrobial phototherapy, e.g., a broad spectrum of action, no resistance, non-invasive and low-cost modality, photosensitizers have been used as a satisfactory alternative for the elimination and inactivation of antibiotic resistant bacteria (ARB), such as methicillin-resistant *Staphylococcus aureus* (MRSA) [22,23], multi-drug resistance *Pseudomonas aeruginosa* [24] and vancomycin-resistant *Enterococcus faecium* [25]. Accordingly, the antimicrobial PDT can be applied in the treatment of skin and soft tissue infections caused by MRSA [26], cystic fibrosis pulmonary infections caused by *P. aeruginosa* [27], and nosocomial infections caused by *E. faecium* [28]. However, the knowledge of the effects of photosensitizers on the horizontal transfer of ARGs and the underlying mechanisms remain elusive. In this study, we evaluated the frequency of transformation mediated by ampicillin resistant plasmid pUC19 and conjugation mediated by multidrug resistant plasmid pRP4 under the exposure to different concentrations and various light-activation durations of a photosensitizer (Visible Light-activated Rose Bengal, VLRB). Additionally, we explored the potential mechanisms of VLRB for the inhibition of horizontal transfer of ARGs by determining the variations in the extracellular plasmid DNA structure, cell membrane permeability, bacterial antioxidant enzyme activities, and mRNA expression levels of conjugative transfer genes. The results will provide data for the development of methods to prevent and control the spread of antimicrobial resistance.

2. Materials and methods

2.1. Photosensitizer, plasmids, competent cells, donor cells, and recipient cells

The visible light-activated photosensitizer (VLRB) was synthesized using Rose Bengal (RB), from Shanghai Aladdin Bio-Chem Technology Co., Ltd according to a previous study [29]. Rose Bengal is an anionic xanthene dye, a derivative of fluorescein. The intrinsic cytotoxicity of RB against tumor and microbial cells accounts for its therapeutic potential, and thus RB has been widely used as a photosensitizer in photodynamic therapy [30,31]. All the chemical reagents were analytical grade, and the deionized water was used to prepare the working solution of VLRB. The visible light system was supported by a 10 W power white LED (DP-1054, Duration Power, China), 4000–4500 K color temperature at an irradiation distance of 12 cm, and the light density was measured in μmol m^{-2} s^{-1} by Quantum sensors (Apogee MQ-510, America). Plasmid pUC19, which confers ampicillin (Amp) resistance, and plasmid pRP4, which carries genes encoding resistance to kanamycin sulfate (Kan), Amp, and tetracycline (Tet), were used to analyze the changes in extracellular plasmid DNA structure after VLRB treatment. In addition, the effects of VLRB on transformation efficiency were determined using *Escherichia coli* DH5α competent cells (Takara, Japan) and plasmid pUC19. Conjugation experiments were performed using the donor strain *Escherichia coli* HB101 carrying the plasmid pRP4 and the recipient strain *Escherichia coli* K12. The recipient *E. coli* K12 is intrinsically resistant to rifampicin (Rif). *Staphylococcus aureus* RN4220 was applied to study the antibacterial effects of VLRB on Gram-positive bacteria. *E. coli* HB101 (RP4) (in 50 mg/L of Tet), *E. coli* K12 (in 100 mg/L of Rif), and *S. aureus* RN4220 were cultured separately overnight at 37 °C in Luria-Bertani (LB) broth with corresponding antibiotics. Mid-logarithmic growth-phase bacterial cells were collected by centrifugation at 6,200 g for 2 min at 25 °C and the resulting cell pellets were washed twice and resuspended with 10 mM sterile phosphate buffer solution (PBS). The concentrations of all strains were adjusted to 10^6 colony-forming units per milliliter (CFU/mL) and 10^9 CFU/mL using sterile PBS, respectively.

2.2. Photodynamic inactivation of bacterial cells

S. aureus RN4220 (10^6 CFU/mL and 10^9 CFU/mL), *E. coli* K12 (10^6

CFU/mL and 10^9 CFU/mL), and *E. coli* HB101 (RP4) (10^6 CFU/mL and 10^9 CFU/mL) were used for the evaluation of photodynamic inactivation of bacterial cells by VLRB. For each strain, 4 mL of bacterial suspension and 40 μL VLRB at a final concentration of 10 μg/mL were mixed in the 12-well black cell culture plates, followed by incubation at 37 °C for 50 min in the dark, after which the mixtures were irradiated with a 280 μmol m^{-2} s^{-1} led for 20 min. Bacterial viability was measured by CFU counting on LB agar with selective antibiotics after incubation at 37 °C for 24 h, and the antibacterial activity was calculated according to formula 1. Each experiment was performed in triplicate.

$$mortality = \frac{colony\ \ count\ \ without\ \ treatment - colony\ \ count\ \ with\ \ treatment}{colony\ \ count\ \ without\ \ treatment} \times 100\% \quad (1)$$

2.3. Morphology and transformation of plasmid

Plasmid pUC19 or pRP4 with a final concentration of 10 ng/μL was incubated with different concentrations (0, 0.01, 0.1, 1, 5, 10, 25, 50, 100, and 200 μg/mL) of VLRB, and the mixtures were irradiated under a 280 μmol m^{-2} s^{-1} led with different exposure times (0, 10, 20, and 30 min). Plasmid fragmentation was checked by agarose gel electrophoresis. The treated plasmids were purified with AMPure XP beads (Beckman Coulter, USA) to remove VLRB. The concentration of the purified plasmids was analyzed by ultraviolet spectrophotometry (NanoDrop Lite, ThermoFisher Scientific, US). Purified pUC19 (1 ng) and 100 μL of *E. coli* DH5α competent cells (Takara, Japan) were used for transformation experiments according to the instruction. The resulting cell suspensions from the transformation experiments were plated on LB plates with 100 mg/L ampicillin and incubated at 37 °C for 24 h. The transformation efficiency was calculated according to formula 2. Each experiment was performed in triplicate.

$$transformation\quad efficiency = \frac{transformant\quad CFU}{\mu g\quad pUC19} \times 100\% \quad (2)$$

2.4. Conjugation assays

Equivalent donors and recipients (2 mL, 10^9 CFU/mL) were mixed in 12-well black cell plates, and VLRB was immediately added with different final concentrations (0, 1, 10, 25, and 50 μg/mL). All treatments were incubated at 37 °C for 50 min in the dark and then irradiated with a 280 μmol m^{-2} s^{-1} led for 30 min. Subsequently, mating experiments were incubated at 25 °C for 8 h. Transconjugants were counted on LB agar plates containing 50 mg/L Tet and 100 mg/L Rif after 24 h incubation at 37 °C. The conjugation frequency was calculated using formula 3. Each experiment was performed in triplicate.

$$conjugation\quad efficiency = \frac{transconjugant\quad concentration}{recipient\quad concentration} \times 100\% \quad (3)$$

To verify whether the transconjugants carried the pRP4, transconjugants were randomly selected, purified, and then cultured in LB broth with 50 mg/L Tet and 100 mg/L Rif overnight. Genomic DNA and plasmids were extracted using the TIANamp Bacteria DNA Kit (Tiangen, China) and TIANprep Mini Plasmid Kit (Tiangen, China), respectively. The pRP4-specific *traG* genes in the extracted plasmid DNA and 16S rRNA gene (16S rRNA-universal) were amplified using PCR. The primers of target genes were listed in Table S1. Each 50 μL PCR reaction contained 25 μL of Master Mix (Thermo Fisher Scientific, USA), 2 μL of forward and reverse primers (10 μM), 1 μL of DNA template, and 22 μL of sterile ddH_2O. The thermal cycle was an initial enzyme activation at 95 °C for 5 min, followed by 30 cycles of denaturation at 95 °C for 30 s, annealing at 55 °C for 30 s, extension at 72 °C for 30 s, and a final extension at 72 °C for 10 min. The presence of plasmid and 16S rRNA gene was detected using 1% agarose gel electrophoresis and then sent for sequencing.

2.5. Cell membrane permeability evaluated by flow cytometry and transmission electron microscopy (TEM)

Overnight cultures of *E. coli* K12 or *E. coli* HB101 (RP4) (4 mL, 10^9 CFU/mL) were transferred to 12-well black cell plates, VLRB was immediately added at different final concentrations (0, 1, 10, 25, and 50 μg/mL). All treatments were incubated at 37 °C in the dark for 50 min followed by light activation with a 280 μmol m^{-2} s^{-1} led for 30 min. Subsequently, the membrane permeability of *E. coli* K12 and *E. coli* HB101 (RP4) was evaluated by flow cytometry (S3e Cell Sorter, Bio-rad, US), respectively. Bacterial viability was measured by a LIVE/DEAD *Bac*Light Bacterial Viability Kit (L7012, ThermoFisher Scientific, US) according to the protocol. Briefly, bacterial cells were diluted to approximately 10^6 CFU/mL using PBS and stained with propidium iodide (PI, 20 mM) or Syto9 (3.34 mM). The boiled cells at 100 °C for 15 min were used as the PI-positive control. After incubation for 15 min in the dark, the stained samples were analyzed by flow cytometry equipped with an excitation wavelength of 488 nm, green fluorescence light (FL-1) (510–540 nm), and red fluorescence light (FL-3) (602–627 nm). All the data were analyzed by Flowjo (version 10) according to previous studies [2,6].

The integrity of cell membranes was evaluated by transmission electron microscopy (TEM) according to previous studies [32,33]. Briefly, bacterial cells were centrifuged, washed, and fixed using 2.5% glutaraldehyde for 2 h. Then, the fixed bacterial cells were rinsed twice with 0.1 M PBS for 10 min, fixed using 0.5% osmic acid for 1 h, dehydrated through a graded series of ethanol (70% ethanol, 10 min; 95% ethanol, 10 min; 100% ethanol, 2 × 10 min), and rinsed with acetone. Samples were subsequently embedded using an Epon 812 substitute, cut on a Leica EM UC7 ultramicrotome, transferred to a 200-mesh copper EM finder grid, and then stained with uranyl acetate. Finally, bacterial cells were examined by a Hitachi H-7650 TEM.

2.6. Bacterial antioxidant enzyme activities

In addition to the VLRB-treated and untreated *E. coli* K12 and *E. coli* HB101 (RP4) solutions that were used in the cell membrane permeability measurement experiments, an additional 1 mL bacterial cells were collected for bacterial antioxidant enzyme activity measurements. The cell disruption was conducted by sonication using 10-s bursts with 20-s cooling intervals for a total of 4 cycles at 200 W [3]. The cellular debris was removed by centrifugation at 10,000 g for 10 min at 4 °C. The supernatant was immediately applied for the enzyme activity assays. Protein concentration was measured by using a BCA protein assay kit (SK3051, Shanghai Sangon Biological Engineering Technology & Services, China). The activities of catalase (CAT) and superoxide dismutase (SOD) were assessed using the kits from Nanjing Jiancheng Institute of Biological Engineering (Nanjing, China) according to the manufacturer's instructions.

2.7. The expression level of conjugative transfer genes

Bacterial RNA was extracted from the cell pellets by using the TRIzol Reagent (Invitrogen, US) according to the manufacturer's instruction. RNA was transcribed to cDNA by reverse transcription polymerase chain reaction (RT-PCR) with a reverse transcription kit (Invitrogen, USA). Real-time PCR was carried out by using SYBR Green I (Takara, Japanese) on a Roche 480 system (LightCycler480II, Germany). Conjugation-related genes of pRP4 including *trfAp* (DNA-transfer-and-replication system), *trbBp* (mating pair formation system), and the genes *korA*, *korB,* and *trbA* (global regulatory system) [3] were qualified with the 16S rRNA gene (16S rRNA-qPCR) as a reference gene. The primer sequences of target genes were listed in Table S1. Real-time PCR was performed in a 20 μL qPCR mixture consisting of 10 μL 2 × LightCycler 480 SYBR

Green I Master, 0.2 μL bovine serum albumin (20 mg/L), 0.8 μL each primer (10 μM), 2 μL template DNA and 6.2 μL nuclease-free PCR-grade water. The reaction conditions were set as follows: an initial denaturation at 95 °C for 5 min, a PCR step of 40 cycles of 95 °C for 30 s, 60 °C for 30 s, and 72 °C for 30 s (signal was collected at the 31 s), and a dissociation stage of 95 °C for 15 s, 60 °C for 1 min, and 95 °C for 15 s

2.8. Statistical analysis

Each experiment was conducted in triplicate. Data were presented as the mean with standard deviation in the figures. All statistical analysis was performed using SPSS Statistic 26 (SPSS, US). Significant differences were assessed using the One-Way analysis of variation (ANOVA), a value of $P < 0.05$ was considered significant.

3. Results

3.1. Structural changes of plasmid and the effects of VLBR on bacterial cell viability

The agarose gel electrophoretic patterns of the VLRB-treated and -untreated plasmids (pUC19 and pRP4) were analyzed to evaluate the effects of VLRB on the structure of plasmid DNA. Bands with different lengths (ranging from 2.0 kb to 4.0 kb) (Form II) and smear bands of pUC19 and pRP4 were observed in VLRB treatment other than the supercoiled plasmid DNA (Form I) (Figs. S1 and S2a). The recovery rate of treated pRP4 by the AMPure XP beads decreased with increased VLRB concentrations compared to non-VLRB control (Fig. S2b). VLRB treatment did not exhibit a fatal effect on *E. coli* K12 or *E. coli* HB101 (RP4) at a cell density of 1.0×10^9 CFU/mL, while 10 μg/mL VLRB was sufficient to kill *S. aureus* RN4220 within 20 min at a light density of 280 μmol m^{-2} s^{-1} (Table S4).

3.2. Decreases in the transformation efficiency

The transformation efficiency of untreated pUC19 was 5.58×10^8 CFU/μg pUC19, which significantly decreased with increased VLRB concentrations and exposure durations ($p < 0.05$), with a maximum of 580-fold decrease after 5 μg/mL VLRB treatment for 20 min (Fig. 1 and Table S3).

3.3. VLRB treatment inhibits the conjugative transfer of pRP4

To evaluate the effects of VLRB treatment on conjugation, we used *E. coli* HB101 with the conjugative plasmid pPR4 as the donor and *E. coli* K12 as the recipient in the conjugation model. Before the conjugation process, the cells were exposed to VLRB at concentrations from 0 to 50 μg/mL, incubated under a dark environment for 50 min, then irradiated with visible light for 30 min. The conjugation frequency of pRP4 significantly decreased ($p < 0.05$) with the increased concentrations of VLRB (Fig. 2), with a maximum of 11-fold decrease from 4.05×10^{-5} to 4.40×10^{-4} in 50 μg/mL VLRB treatment (Fig. 2). The plasmid DNA extracted from the transconjugants showed the same size as that of pRP4 extracted from the donors (Fig. S3a), and the amplifications of the *traG* gene of pRP4 were all positive from the randomly picked transconjugants (Fig. S3b). The sequences of full-length 16S rRNA further showed that the transconjugants were *E. coli* K12.

3.4. Variations in the integrity of cell membranes

The effects of different concentrations of VLRB on the membrane permeability of *E. coli* HB101 (RP4) and *E. coli* K12 were shown in Fig. 3 and Fig. S4. Generally, under VLRB treatment, the fluorescence intensity of PI increased in both strains, indicating elevated cell membrane permeability. A significant increase in the percentage of PI-positive cells

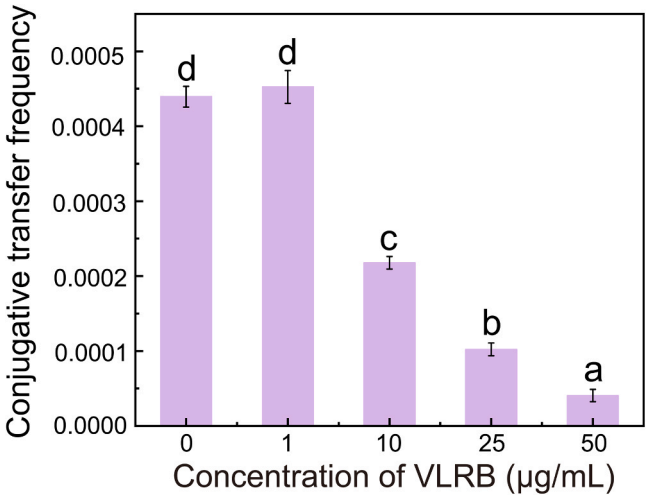

Fig. 2. Effects of VLRB on the conjugative transfer frequency of pRP4 at different concentrations (0, 1, 10, 25, and 50 μg/mL) under visible light irradiation (at power tensity of 280 μmol m^{-2} s^{-1}, 30 min).

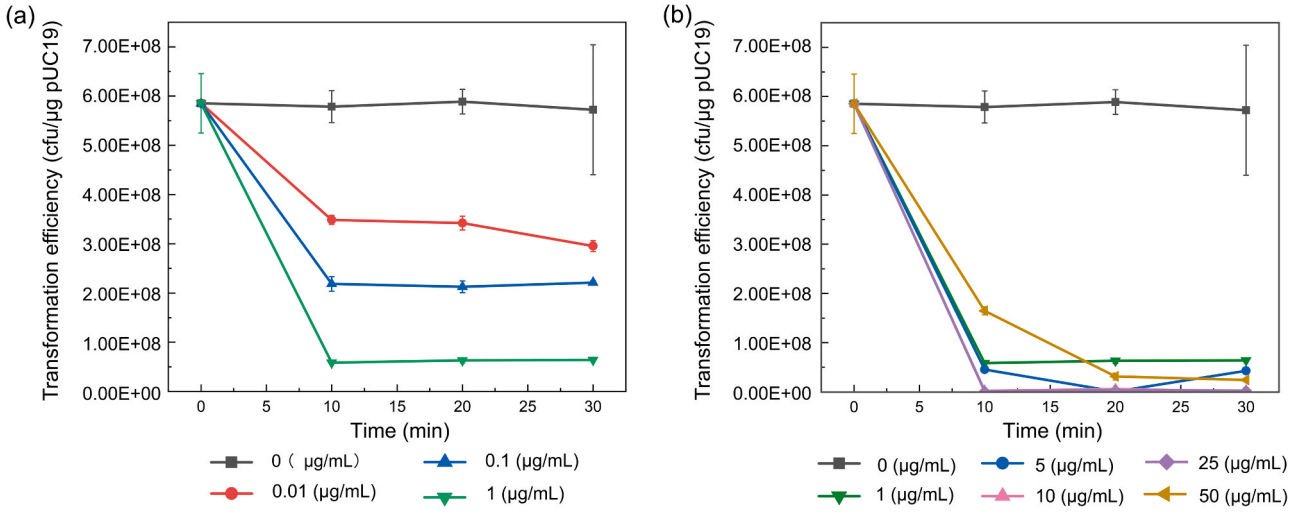

Fig. 1. Changes in the transformation efficiency of pUC19 when exposed to different concentrations (0, 0.01, 0.1, 1, 5, 10, 25, and 50 μg/mL) and different treatment times (0, 10, 20, and 30 min) of VLRB.

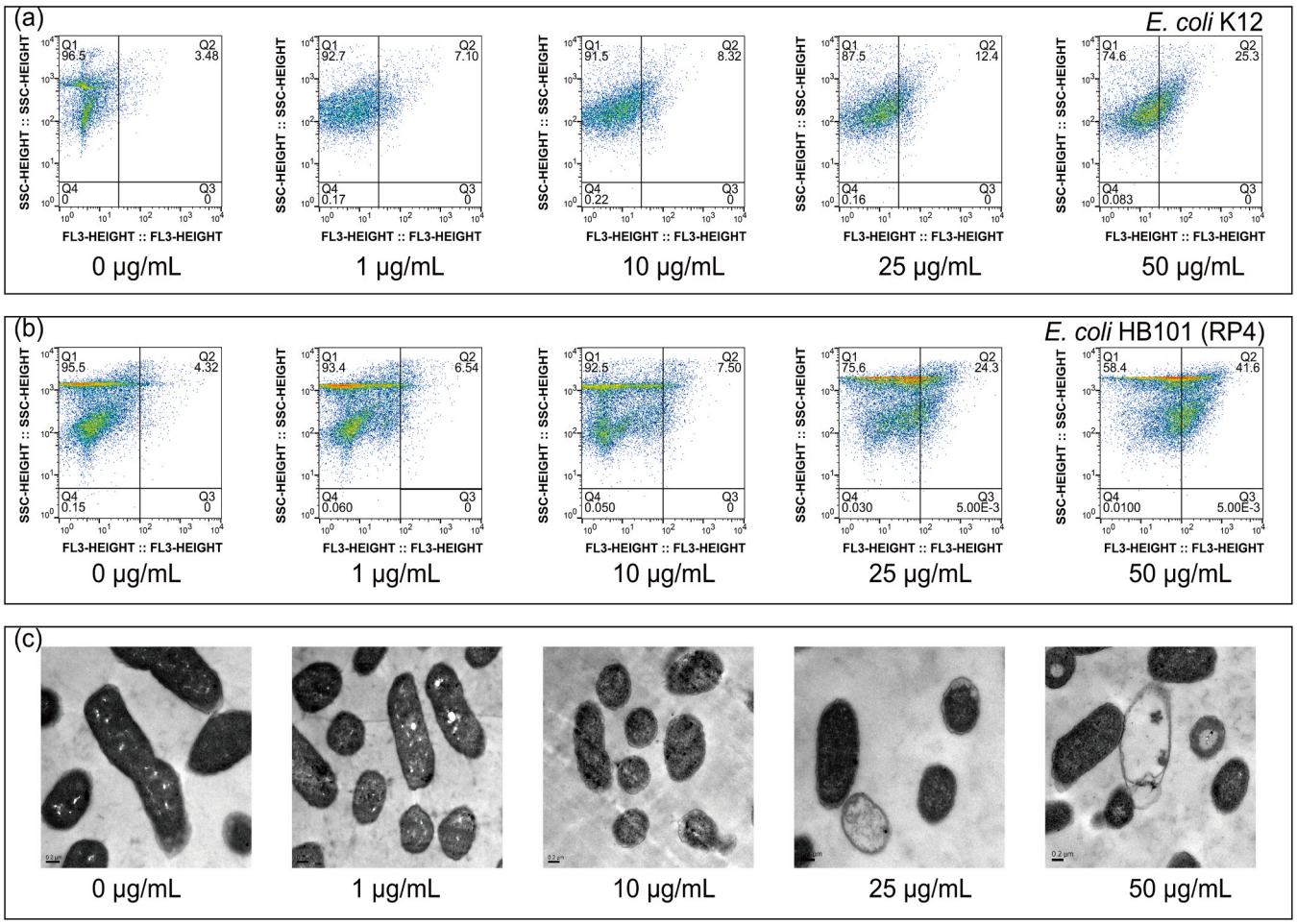

Fig. 3. The dot plots of *E. coli* K12 (a) and *E. coli* HB101 (RP4) (b) membrane permeability treated by VLRB, the dot in the up-right area represents PI-positive cell (permeable membranes, with high membrane permeability) and the dot in the up-left area represents PI-negative cell (intact membranes, with normal membrane permeability). TEM photos of *E. coli* K12 and *E. coli* HB101 (RP4) treated with or without VLRB addition after 30 min in the light tensity of 280 μmol m^{-2} s^{-1} (Scale bars, 200 nm) (c).

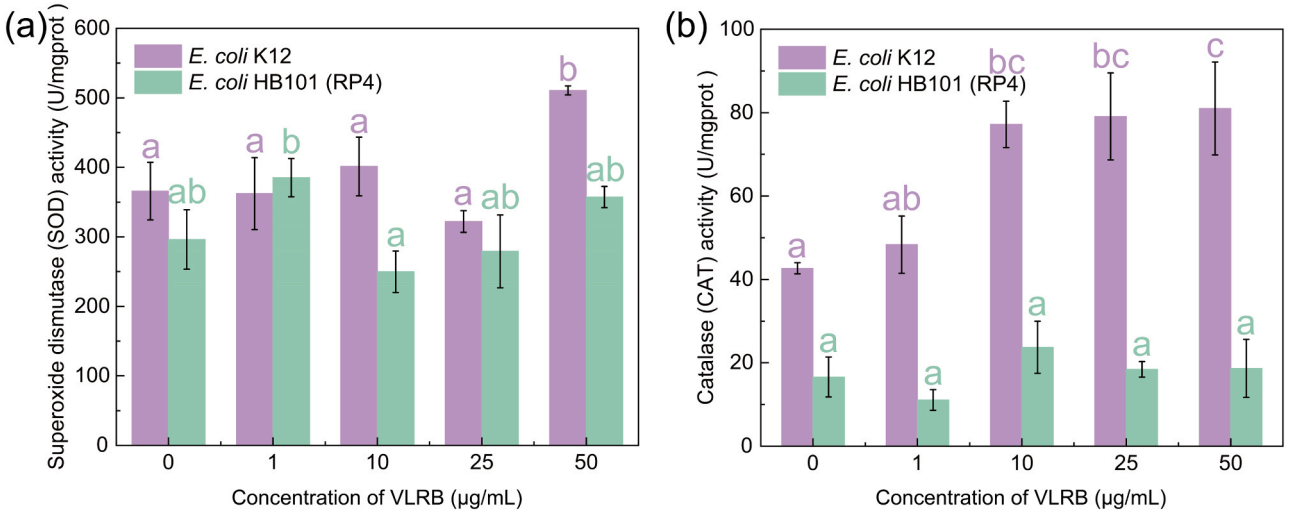

Fig. 4. The effects of different concentrations VLRB treatment on the activity of SOD (a) and CAT (b) of *E. coli* K12 or *E. coli* HB101 (RP4) under 280 μmol m^{-2} s^{-1} and 30 min of light. Different letters indicate significant differences at the $P < 0.05$ level (ANOVA).

was observed when bacterial cells were exposed to > 10 μg/mL VLRB ($P < 0.01$) (Fig. 3 and Fig. S4). Furthermore, bacterial cell morphology by TEM revealed that without VLRB treatment, the cell membranes of *E. coli* K12 and *E. coli* HB101 (RP4) were intact with smooth and clear cell borders (Fig. 3c). However, the bacterial cell membranes were partially damaged, and noticeable protrusions were observed with the

addition of VLRB, even pored cell membranes appeared following high-concentration VLRB treatment.

3.5. Effects of VLRB on bacterial oxidative stress-response systems

The oxidative stress-response systems of bacteria were affected when treated with VLRB at different concentrations. Notably, the activity of SOD of *E. coli* K12 was significantly increased when treated with a high concentration of VLRB (50 μg/mL) ($P < 0.05$); while there was no significant variation of *E. coli* HB101 (RP4) under the treatment of VLRB (Fig. 4a). The CAT activity of *E. coli* K12 significantly increased with VLRB concentrations ($P < 0.05$), whereas a significant difference was not observed in *E. coli* HB101 (RP4) after VLRB treatment (Fig. 4b).

3.6. Expression level of conjugation-related genes

The broad-host-range plasmid pRP4 is a typical IncP α-type plasmid, and its conjugative transfer ability depends on the expression of conjugation genes and corresponding regulatory genes. The expression level of Dtr genes *trfAp* and *trbBp* significantly decreased with the increasing VLRB concentrations (Figs. 5a and 5b), suggesting that VLRB treatment could inhibit the formation of mating pairs and the replication of pPR4. Meanwhile, in comparison with the control, the expression levels of the global regulator genes *korA*, *korB* and *trbA* increased by 9.38-fold, 7.30-fold and 11.94-fold, respectively, when the cultures were exposed to 1 μg/mL VLRB (Fig. 5c). These results confirmed that the repressed expression of *trfAp* and *trbBp* resulted in the deduction of pRP4 conjugation efficiency.

4. Discussion

The global spread of ARGs has led to the failure of antibiotic therapy, and consequently prolonged hospitalization and increased mortality of patients [34]. Plasmid-mediated gene transfer is one of the major drivers for the transmission of ARGs among microorganisms. Photosensitizer has been adopted in the treatment of non-neoplastic disease, various cancer types [35,36], and bacterial infections [37-39]. Based on the established transformation and conjugation models, our results indicated that the photosensitizer (VLRB) could suppress the plasmid-encoded ARG transfer by inhibiting transformation and conjugation, and thus has the potential to mitigate the dissemination of ARGs in the environments. We collected multiple pieces of evidence, including changes in plasmid conformation, cell membrane permeability, antioxidant enzyme activities, and transcriptional responses to elucidate the underlying mechanisms.

Transformation occurs when competent bacteria take up extracellular DNA, especially plasmid DNA, contributing to the dissemination of antibiotic resistance and the emergence of antibiotic resistant pathogenic bacteria. To rule out the potentially detrimental effects of VLRB on the competent cells, the plasmids were purified after VLRB treatment before transformation experiments. Our results showed that the transformation efficiency of treated pUC19 significantly decreased with increasing concentrations of VLRB (Fig. 1). The configuration of plasmid DNA is one of the key factors influencing transformation efficiency. Supercoiled plasmids are much easier to enter bacterial cells owing to their compact conformation than open circular and linear forms [40,41]. Typically, plasmid in linear form shows up as a larger band on the agarose gel than in supercoiled form, which moves faster in the agarose gel [41]. The occurrence of smeared bands (Figs. S1 and S2a) after the treatment of VLRB, indicating that VLRB treatment caused structural modification of the supercoiled plasmid, resulted in the formation of the linear plasmid. Additionally, the recovery rate of treated pRP4 was decreased with the increasing VLRB concentration (Fig. S2b), indicating a dose-dependent effect of VLRB on DNA. Photodynamic process typically generates enormous reactive intermediates (•OH and $^1O_2$), and the oxidative stress has been reported to result in DNA damage, including strand breaks, base modification, and deoxyribose degradation, which would lead to structural changes of plasmid [42,41,43], thus affecting the transformation efficiency. Previous studies have also shown that •OH would non-selectively oxidize DNA bases, leading to the break of DNA strands by extracting •H from the sugar moiety of DNA [43,44], and $^1O_2$ could selectively oxidize guanine, further enhancing the damage of DNA [43,45]. Furthermore, damages to the promoter or open reading frame of plasmid-encoded ARGs may lead to transformant colonization failure and reduced transformation efficiency. These data indicated that the VLRB affected the morphology or structure of

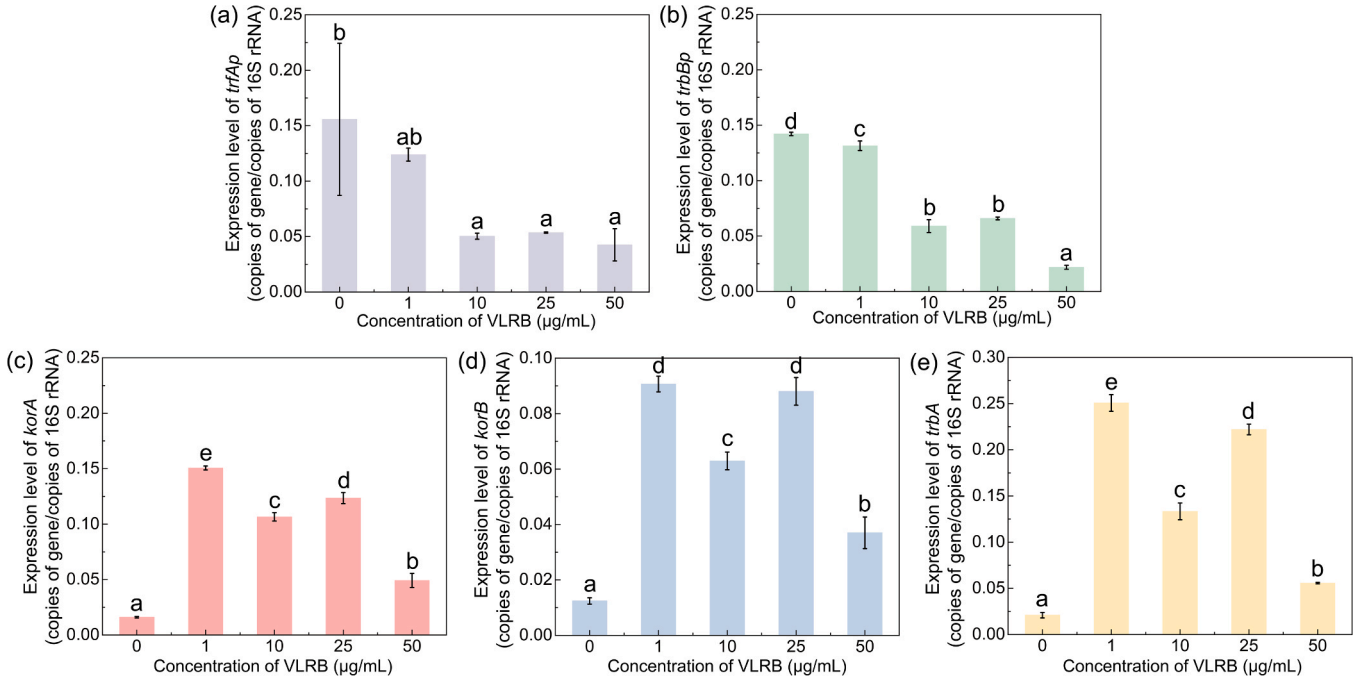

Fig. 5. The effects of VLRB treatments on the expression of global regulatory genes (Grg, including *korA*, *korB* and *trbA*), mating pair formation genes (Mpf, *trbBp*) and DNA-transfer-and-replication genes (Dtr, *trfAp*). Different letters indicate significant differences at the $P < 0.05$ level (ANOVA).

plasmids, and consequently reduced the frequency of transformation [41,43].

VLRB treatment did not affect the viability of *E. coli* K12 or *E. coli* HB101 (RP4), which belong to Gram-negative bacteria, whereas 10 μg/mL of VLRB was sufficient to kill *S. aureus* RN4220 (Gram-positive bacteria) within 20 min at a light density of 280 μmol m^{-2} s^{-1} (Table S4), indicating that VLRB does not have bactericidal ability against donor and recipient bacteria. Additionally, the conjugative transfer frequency of pRP4 significantly decreased ($p < 0.05$) with the increasing concentrations of VLRB (Fig. 2a), and the cell membrane permeability, antioxidant enzyme activities, and conjugative corresponding gene expression levels were significantly influenced during the photodynamic process, suggesting that VLRB activated by visible light can affect the conjugation of bacteria through altering bacterial physiology, biochemistry, and gene expression, instead of killing the bacterial cells directly.

Photodynamic reactions of photosensitizers may prevent the conjugative transfer of antibiotic resistant plasmid by affecting the physiological and biochemical characteristics of both donor and recipient bacterial strains [46,47]. In this study, elevated cell membrane permeability was detected in both donor (*E. coli* HB101 (RP4)) and recipient (*E. coli* K12) cells under the exposure to VLRB (Figs. 3a and 3b), which was consistent with the observations by TEM (Fig. 3c). Several previous studies have demonstrated that many chemicals, such as nanoalumina [3], preservatives [2], ionic liquid [48], nonnutritive sweeteners [5], cadmium, and iron oxide nanoparticles [49], can affect bacterial membrane permeability by changing the membrane compositions and structures. Bacteria can alter their membrane permeability by regulating the expression of outer membrane proteins as well [50,51]. A significant increase in the CAT activity was observed in *E. coli* K12 but not in *E. coli* HB101 (RP4), indicating that the bacterial SOS response was triggered in *E. coli* K12, and intracellular ROS could accumulate when VLRB was activated. The difference between donor and recipient bacteria in the response to ROS was consistent with precious studies [52,53] and could be attributed to the regulation of SOS response-related genes which was associated with *parDE*-type toxin-antitoxin system encoded by pRP4 in the donor *E. coli* HB101 [54].

However, in contrast to our finding, assorted studies have indicated that many compounds, e.g., artificial sweeteners [5], preservatives [2], and gibberellin [53], can facilitate the conjugative transfer of ARGs by triggering intracellular ROS overproduction and increasing membrane permeability. The discrepancy could be attributed to the production of massive extracellular ROS and free radicals following visible light excitation of VLRB. The zeta potentials and hydrodynamic diameter of bacterial cells would decrease after free radical exposure, resulting in a significant reduction in the aggregation of cells, and consequently weakening the physical contact between cells [55-57]. In addition, previous studies indicated that prolonged exposure to extracellular ROS and free radicals could depress the expression of genes related to adenosine-triphosphate synthesis and pilin production, thereby inhibit the conjugative transfer of pRP4 [56,58,59].

The photodynamic process of photosensitizers can decrease conjugation efficiency by regulating the expression of conjugation-related genes. The Grg system (*korA*, *korB*, and *trbA*) acts as global regulator in plasmid replication, transfer, and stable inheritance [60], and the Mpf system (*trbBp*) is responsible for the formation of channels or pores at the mating bridge between donor and recipient bacteria [61,62]. In addition, the Dtr system (*trfAp*) is associated with the ralaxosome formation during the transfer-replication process [62]. In this study, we found that the expression of *korA*, *korB,* and *trbA* was significantly enhanced with the VLRB treatment, whereas the expression of *trfAp* and *trbBp* was repressed significantly (Fig. 5), while when VLRB concentration was less than 10 μg/mL, a significant decrease in the expression levels of *trfAp* and *trbBp* was not observed. These results suggested that the photodynamic process of VLRB inhibited the formation of mating pairs by restraining the mating bridge and relaxosome formation during the transfer-replication process, which further contributed to the reduced conjugative transfer frequency after the treatment of VLRB.

The VLRB was synthesized from Rose Bengal, characterized by high hydrophilicity, sensitivity, antibacterial activity, and stability [63,64], and its anionic charge prevents the uptake of cells [63], demonstrating to be promising in the biomedical field. Furthermore, in contrast to the irradiation of light with specific wavelengths for PDT, the visible light used in VLRB activation has the advantages of a higher level of perfusion, lower thermal stress, and easy availability. Moreover, combining VLRB with other materials, such as antibiotics [65], ultrasound irradiation [66], nanoparticles [67], and chlorhexidine [68] may show higher capacity in inhibiting the propagation of ARGs.

5. Conclusion

This study revealed that the efficiency of transformation and conjugation of antibiotic resistant plasmids significantly decreased under exposure to VLRB. Photodynamic activation of VLRB can induce photodegradation of plasmid (plasmid strand breaks and base oxidization), leading to the changes in the plasmid conformation and reduction in the transformation efficiency. Furthermore, VLRB exposure could generate a mass of extracellular ROS, facilitating the oxidative damage of cells and affecting the expression of conjugation-related genes, and thus decrease the conjugative transfer of plasmid. Photosensitizers have been demonstrated with germicidal effects on Gram-positive bacteria including *S. aureus* [69], *Bacillus cereus* [70], *Enterococcus faecalis* [71], *Streptococcus mutans* [72], et al., our findings expanding the roles of photosensitizers in the inhibition of plasmid-mediated HGT in Gram-negative bacteria, which could be utilized for the prevention and control of the spread of plasmid-encoded ARGs. Nevertheless, the plasmid-mediated transformation and conjugation experiments were conducted using *E. coli* strains, more bacterial strains should be included to test the robustness of VLRB.

CRediT authorship contribution statement

Yan-Zi Wang: Investigation, Conceptualization, Methodology, Data curation, Formal analysis, Writing. **Xin-Li An:** Methodology, Writing – review & editing. **Xiao-Ting Fan:** Investigation, Methodology, Writing – review & editing. **Qiang Pu:** Investigation, Methodology. **Hu-Li:** Methodology, Data curation. **Wen-Zhen Liu:** Investigation. **Zhuo Chen:** Supervision, Funding acquisition. **Jian-Qiang Su:** Conceptualization, Supervision, Project administration, Funding acquisition, Writing – review & editing.

Declaration of Competing Interest

The authors declare that they have no known competing financial interests or personal relationships that could have appeared to influence the work reported in this paper.

Data availability

Data will be made available on request.

Acknowledgements

This study was financially supported by the National Key Research and Development Plan (2020YFC1806902), the National Natural Science Foundation of China (81991535, 21936006, and 32061143015), and the FJIRSM&IUE Joint Research Fund (RHZX-2018-004). We thank Hong-Yun Ren for her assistance in preparation of samples for TEM.

Appendix A. Supporting information

Supplementary data associated with this article can be found in the online version at doi:10.1016/j.jhazmat.2023.132564.

References

[1] Thomas, C.M., Nielsen, K.M., 2005. Mechanisms of, and barriers to, horizontal gene transfer between bacteria. Nat Rev Microbiol 3, 711–721. https://doi.org/10.1038/nrmicro1234.

[2] Cen, T., Zhang, X., Xie, S., Li, D., 2020. Preservatives accelerate the horizontal transfer of plasmid-mediated antimicrobial resistance genes via differential mechanisms. Environ Int 138, 105544. https://doi.org/10.1016/j.envint.2020.105544.

[3] Qiu, Z., Yu, Y., Chen, Z., Jin, M., Yang, D., Zhao, Z., et al., 2012. Nanoalumina promotes the horizontal transfer of multiresistance genes mediated by plasmids across genera. Proc Natl Acad Sci USA 109, 4944–4949. https://doi.org/10.1073/pnas.1107254109.

[4] Wang, Y., Lu, J., Engelstadter, J., Zhang, S., Ding, P., Mao, L., et al., 2020. Non-antibiotic pharmaceuticals enhance the transmission of exogenous antibiotic resistance genes through bacterial transformation. ISME J 14, 2179–2196. https://doi.org/10.1038/s41396-020-0679-2.

[5] Yu, Z., Wang, Y., Lu, J., Bond, P.L., Guo, J., 2021. Nonnutritive sweeteners can promote the dissemination of antibiotic resistance through conjugative gene transfer. ISME J 15, 2117–2130. https://doi.org/10.1038/s41396-021-00909-x.

[6] Zhang, Y., Gu, A.Z., He, M., Li, D., Chen, J., 2017. Subinhibitory concentrations of disinfectants promote the horizontal transfer of multidrug resistance genes within and across genera. Environ Sci Technol 51, 570–580. https://doi.org/10.1021/acs.est.6b03132.

[7] Getino, M., de da Cruz, F., 2018. Natural and artificial strategies to control the conjugative transmission of plasmids. Microbiol Spectr 6. https://doi.org/10.1128/microbiolspec.MTBP-0015-2016.

[8] Getino, M., Sanabria-Rios, D.J., Fernandez-Lopez, R., Campos-Gomez, J., Sanchez-Lopez, J.M., Fernandez, A., et al., 2015. Synthetic fatty acids prevent plasmid-mediated horizontal gene transfer. Mbio 6. https://doi.org/10.1128/mBio.01032-15.

[9] Palencia-Gandara, C., Getino, M., Moyano, G., Redondo, S., Fernandez-Lopez, R., Gonzalez-Zorn, B., et al., 2021. Conjugation inhibitors effectively prevent plasmid transmission in natural environments. mBio 12, e0127721. https://doi.org/10.1128/mBio.01277-21.

[10] Agostinis, P., Berg, K., Cengel, K.A., Foster, T.H., Girotti, A.W., Gollnick, S.O., et al., 2011. Photodynamic therapy of cancer: an update. Ca-a Cancer J Clin 61, 250–281. https://doi.org/10.3322/caac.20114.

[11] Tan, Z., Zhang, J.D., Lin, L.S., Li, B.H., 2016. Quantification of reactive oxygen species for photodynamic therapy. Conference on Optics in Health Care and Biomedical Optics VII. 0024. PEOPLES R CHINA, Beijing.

[12] Zhao, J.Z., Wu, W.H., Sun, J.F., Guo, S., 2013. Triplet photosensitizers: from molecular design to applications. Chem Soc Rev 42, 5323–5351. https://doi.org/10.1039/c3cs35531d.

[13] Chen, R.H., Huang, S.S., Lin, T.T., Ma, H.S., Shan, W.J., Duan, F., et al., 2021. Photoacoustic molecular imaging-escorted adipose photodynamic-browning synergy for fighting obesity with virus-like complexes. Nat Nanotechnol 16, 455. https://doi.org/10.1038/s41565-020-00844-6.

[14] Li, X.S., Lovell, J.F., Yoon, J., Chen, X.Y., 2020. Clinical development and potential of photothermal and photodynamic therapies for cancer. Nat Rev Clin Oncol 17, 657–674. https://doi.org/10.1038/s41571-020-0410-2.

[15] Sultan, A.A., Jerjes, W., Berg, K., Hogset, A., Mosse, C.A., Hamoudi, R., et al., 2016. Disulfonated tetraphenyl chlorin (TPCS2a)-induced photochemical internalisation of bleomycin in patients with solid malignancies: a phase 1, dose-escalation, first-in-man trial. Lancet Oncol 17, 1217–1229. https://doi.org/10.1016/s1470-2045(16)30224-8.

[16] Yang, Y., Huang, J.S., Wei, W., Zeng, Q., Li, X.P., Xing, D., et al., 2022. Switching the NIR upconversion of nanoparticles for the orthogonal activation of photoacoustic imaging and phototherapy. Nat Commun 13. https://doi.org/10.1038/s41467-022-30713-w.

[17] Zhang, Y.Y., Tian, S.D., Huang, L.P., Li, Y.A., Lu, Y., Li, H.Y., et al., 2022. Reactive oxygen species-responsive and Raman-traceable hydrogel combining photodynamic and immune therapy for postsurgical cancer treatment. Nat Commun 13. https://doi.org/10.1038/s41467-022-32160-z.

[18] Kwiatkowski, S., Knap, B., Przystupski, D., Saczko, J., Kedzierska, E., Knap-Czop, K., et al., 2018. Photodynamic therapy - mechanisms, photosensitizers and combinations. Biomed Pharmacother 106, 1098–1107. https://doi.org/10.1016/j.biopha.2018.07.049.

[19] Oyim, J., Omolo, C.A., Amuhaya, E.K., 2021. Photodynamic antimicrobial chemotherapy: advancements in porphyrin-based photosensitize development. Front Chem 9. https://doi.org/10.3389/fchem.2021.635344.

[20] Yu, C., Wang, N., Chen, X., Jiang, Y., Luan, Y., Qin, W., et al., 2023. A photodynamic-mediated glutamine metabolic intervention nanodrug for triple negative breast cancer therapy. Mater Today Bio 19. https://doi.org/10.1016/j.mtbio.2023.100577.

[21] Ghorbani, J., Rahban, D., Aghamiri, S., Teymouri, A., Bahador, A., 2018. Photosensitizers in antibacterial photodynamic therapy: an overview. Laser Ther 27, 293–302. https://doi.org/10.5978/islsm.27_18-RA-01.

[22] Arenas, Y., Monro, S., Shi, G., Mandel, A., McFarland, S., Lilge, L., 2013. Photodynamic inactivation of *Staphylococcus aureus* and methicillin-resistant *Staphylococcus aureus* with Ru (II)-based type I/type II photosensitizers. Photo Photodyn Ther 10, 615–625. https://doi.org/10.1016/j.pdpdt.2013.07.001.

[23] Fu, X.-J., Zhu, Y.-Q., Peng, Y.-B., Chen, Y.-S., Hu, Y.-P., Lu, H.-X., et al., 2014. Enzyme activated photodynamic therapy for methicillin-resistant *Staphylococcus aureus* infection both in vitro and in vivo. J Photochem Photobiol B-Biol 136, 72–80. https://doi.org/10.1016/j.jphotobiol.2014.04.016.

[24] Tseng, S.P., Teng, L.J., Chen, C.T., Lo, T.H., Hung, W.C., Chen, H.J., et al., 2009. Toluidine blue O photodynamic inactivation on multidrug-resistant *Pseudomonas aeruginosa*. Lasers Surg Med 41, 391–397. https://doi.org/10.1002/lsm.20765.

[25] Chibebe Junior, J., Fuchs, B.B., Sabino, C.P., Junqueira, J.C., Jorge, A.O.C., Ribeiro, M.S., et al., 2013. Photodynamic and antibiotic therapy impair the pathogenesis of *Enterococcus faecium* in a whole animal insect model. PLoS ONE 8, 1–10. https://doi.org/10.1371/journal.pone.0055926.

[26] Drury, S.L., Miller, A.R., Laut, C.L., Walter, A.B., Bennett, M.R., Su, M., et al., 2021. Simultaneous exposure to intracellular and extracellular photosensitizers for the treatment of *Staphylococcus aureus* infections. Antimicrob Agents Chemother 65, e0091921. https://doi.org/10.1128/AAC.00919-21.

[27] Donnelly, R.F., McCarron, P.A., Cassidy, C.M., Elborn, J.S., Tunney, M.M., 2007. Delivery of photosensitisers and light through mucus: investigations into the potential use of photodynamic therapy for treatment of *Pseudomonas aeruginosa* cystic fibrosis pulmonary infection. J Control Release 117, 217–226. https://doi.org/10.1016/j.jconrel.2006.11.010.

[28] Wozniak, A., Kruszewska, B., Pieranski, M.K., Rychlowski, M., Grinholc, M., 2021. Antimicrobial photodynamic inactivation affects the antibiotic susceptibility of *Enterococcus* spp. clinical isolates in biofilm and planktonic cultures. Biomolecules 11. https://doi.org/10.3390/biom11050693.

[29] Liu, W.Z., Zhang, Y.X., You, W.W., Su, J.Q., Yu, S.H., Dai, T., et al., 2020. Near-infrared-excited upconversion photodynamic therapy of extensively drug-resistant *Acinetobacter baumannii* based on lanthanide nanoparticles. Nanoscale 12, 13948–13957. https://doi.org/10.1039/d0nr01073a.

[30] Demartis, S., Obinu, A., Gavini, E., Giunchedi, P., Rassu, G., 2021. Nanotechnology-based Rose Bengal: a broad-spectrum biomedical tool. Dyes Pigments 188. https://doi.org/10.1016/j.dyepig.2021.109236.

[31] Dubey, T., Gorantla, N.V., Chandrashekara, K.T., Chinnathambi, S., 2020. Photodynamic exposure of Rose-Bengal inhibits Tau aggregation and modulates cytoskeletal network in neuronal cells. Sci Rep 10. https://doi.org/10.1038/s41598-020-69403-2.

[32] Graham, L., Orenstein, J.M., 2007. Processing tissue and cells for transmission electron microscopy in diagnostic pathology and research. Nat Protoc 2, 2439–2450. https://doi.org/10.1038/nprot.2007.304.

[33] Shi, Q.Y., Zhang, H., Wang, C.L., Ren, H.Y., Yan, C.Z., Zhang, X., et al., 2020. Bioaccumulation, biodistribution, and depuration of C-13-labelled fullerenols in zebrafish through dietary exposure. Ecotoxicol Environ Saf 191. https://doi.org/10.1016/j.ecoenv.2020.110173.

[34] Berendonk, T.U., Manaia, C.M., Merlin, C., Fatta-Kassinos, D., Cytryn, E., Walsh, F., et al., 2015. Tackling antibiotic resistance: the environmental framework. Nat Rev Microbiol 13, 310–317. https://doi.org/10.1038/nrmicro3439.

[35] Kubrak, T.P., Kolodziej, P., Sawicki, J., Mazur, A., Koziorowska, K., Aebisher, D., 2022. Some natural photosensitizers and their medicinal properties for use in photodynamic therapy. Molecules 27. https://doi.org/10.3390/molecules27041192.

[36] Zhao, C.Q., Rehman, F.U., Jiang, H., Selke, M., Wang, X.M., Liu, C.Y., 2016. Titanium dioxide-tetra sulphonatophenyl porphyrin nanocomposites for target cellular bio-imaging and treatment of rheumatoid arthritis. Sci China-Chem 59, 637–642. https://doi.org/10.1007/s11426.016-5568-1.

[37] Anas, A., Sobhanan, J., Sulfiya, K.M., Jasmin, C., Sreelakshmi, P.K., Biju, V., 2021. Advances in photodynamic antimicrobial chemotherapy. J Photochem Photobiol C-Photochem Rev 49. https://doi.org/10.1016/j.jphotochemrev.2021.100452.

[38] Jori, G., Fabris, C., Soncin, M., Ferro, S., Coppellotti, O., Dei, D., et al., 2006. Photodynamic therapy in the treatment of microbial infections: basic principles and perspective applications. Lasers Surg Med 38, 468–481. https://doi.org/10.1002/lsm.20361.

[39] Yu, C., Gao, Y.C., Zhang, Y.L., Wang, J., Zhang, Y.F., Li, J., et al., 2021. A targeted photosensitizer mediated by visible light for efficient therapy of bacterial keratitis. Biomacromolecules 22, 3704–3717. https://doi.org/10.1021/acs.biomac.1c00461.

[40] Hanahan, D., 1983. Studies on transformation of *Escherichia coli* with plasmids. J Mol Biol 166, 557–580. https://doi.org/10.1016/s0022-2836 (83)80284-8.

[41] Lee, G.J., Choi, M.A., Kim, D., Kim, J.Y., Ghimire, B., Choi, E.H., et al., 2017. Influence of plasma-generated reactive species on the plasmid DNA structure and plasmid-mediated transformation of *Escherichia coli* cells. J Appl Phys 122. https://doi.org/10.1063/1.4991081.

[42] Imlay, J.A., Linn, S., 1988. DNA damage and oxygen radical toxicity. Science 240, 1302–1309. https://doi.org/10.1126/science.3287616.

[43] Zhang, X., Li, J., Fan, W.Y., Yao, M.C., Yuan, L., Sheng, G.P., 2019. Enhanced photodegradation of extracellular antibiotic resistance genes by dissolved organic matter photosensitization. Environ Sci Technol 53, 10732–10740. https://doi.org/10.1021/acs.est.9b03096.

[44] Dizdaroglu, M., 2012. Oxidatively induced DNA damage: mechanisms, repair and disease. Cancer Lett 327, 26–47. https://doi.org/10.1016/j.canlet.2012.01.016.

[45] Agnez-Lima, L.F., Melo, J.T.A., Silva, A.E., Oliveira, A.H.S., Timoteo, A.R.S., Lima-Bessa, K.M., et al., 2012. DNA damage by singlet oxygen and cellular protective mechanisms. Mutat Res-Rev Mutat Res 751, 15–28. https://doi.org/10.1016/j.mrrev.2011.12.005.

[46] Cai, Y., Liu, J., Li, G., Wong, P.K., An, T., 2022. Formation mechanisms of viable but nonculturable bacteria through induction by light-based disinfection and their antibiotic resistance gene transfer risk: a review. Crit Rev Environ Sci Technol 52, 3651–3688. https://doi.org/10.1080/10643389.2021.1932397.

[47] Chen, X., Yin, H., Li, G., Wang, W., Wong, P.K., Zhao, H., et al., 2019. Antibiotic-resistance gene transfer in antibiotic-resistance bacteria under different light irradiation: implications from oxidative stress and gene expression. Water Res 149, 282–291. https://doi.org/10.1016/j.watres.2018.11.019.

[48] Wang, Q., Mao, D., Luo, Y., 2015. Ionic liquid facilitates the conjugative transfer of antibiotic resistance genes mediated by plasmid RP4. Environ Sci Technol 49, 8731–8740. https://doi.org/10.1021/acs.est.5b01129.
[49] Pu, Q., Fan, X.T., Sun, A.Q., Pan, T., Li, H., Lassen, S.B., et al., 2021. Co-effect of cadmium and iron oxide nanoparticles on plasmid-mediated conjugative transfer of antibiotic resistance genes. Environ Int 152. https://doi.org/10.1016/j.envint.2021.106453.
[50] Garvey, N., Stjohn, A.C., Witkin, E.M., 1985. Evidence for RecA protein association with the cell membrane and for changes in the levels of major outer membrane proteins in SOS-induced *Escherichia coli* cells. J Bacteriol 163, 870–876. https://doi.org/10.1128/jb.163.3.870-876.1985.
[51] Wu, S., Ren, P., Wu, Y., Liu, J., Huang, Q., Cai, P., 2022. Effects of hematite on the dissemination of antibiotic resistance in pathogens and underlying mechanisms. J Hazard Mater 431. https://doi.org/10.1016/j.jhazmat.2022.128537.
[52] Zhang, S., Sun, W.-L., Song, H.-L., Zhang, T., Yin, M., Wang, Q., et al., 2022. Effects of voltage on the emergence and spread of antibiotic resistance genes in microbial electrolysis cells: from mutation to horizontal gene transfer. Chemosphere 291. https://doi.org/10.1016/j.chemosphere.2021.132703.
[53] Zhao, H., Liu, X.Y., Sun, Y.L., Liu, J., Waigi, M.G., 2023. Effects and mechanisms of plant growth regulators on horizontal transfer of antibiotic resistance genes through plasmid-mediated conjugation. Chemosphere 318. https://doi.org/10.1016/j.chemosphere.2023.137997.
[54] Hall, J.P.J., Brockhurst, M.A., Dytham, C., Harrison, E., 2017. The evolution of plasmid stability: are infectious transmission and compensatory evolution competing evolutionary trajectories? Plasmid 91, 90–95. https://doi.org/10.1016/j.plasmid.2017.04.003.
[55] Klodzinska, E., Szumski, M., Dziubakiewicz, E., Hrynkiewicz, K., Skwarek, E., Janusz, W., et al., 2010. Effect of zeta potential value on bacterial behavior during electrophoretic separation. Electrophoresis 31, 1590–1596. https://doi.org/10.1002/elps.200900559.
[56] Li, H., Song, R., Wang, Y., Zhong, R., Wang, T., Jia, H., et al., 2021. Environmental free radicals efficiently inhibit the conjugative transfer of antibiotic resistance by altering cellular metabolism and plasmid transfer. Water Res 209, 117946. https://doi.org/10.1016/j.watres.2021.117946.
[57] Maillard, A., Espeche, J.C., Maturana, P., Cutro, A.C., Hollmann, A., 2021. Zeta potential beyond materials science: applications to bacterial systems and to the development of novel antimicrobials. Biochim Et Biophys Acta-Biomembr 1863. https://doi.org/10.1016/j.bbamem.2021.183597.
[58] Meng, X.F., Guan, J.W., Lai, S.S., Fang, L.M., Su, J.Y., 2022. pH-responsive curcumin-based nanoscale ZIF-8 combining chemophotodynamic therapy for excellent antibacterial activity. RSC Adv 12, 10005–10013. https://doi.org/10.1039/d1ra09450e.
[59] Yu, K., Chen, F., Yue, L., Luo, Y., Wang, Z., Xing, B., 2020. CeO_2 nanoparticles regulate the propagation of antibiotic resistance genes by altering cellular contact and plasmid transfer. Environ Sci Technol 54, 10012–10021. https://doi.org/10.1021/acs.est.0c01870.
[60] Kostelidou, K., Jones, A.C., Thomas, C.M., 1999. Conserved C-terminal region of global repressor *KorA* of broad-host-range plasmid RK2 is required for co-operativity between *KorA* and a second RK2 global regulator, *KorB*. J Mol Biol 289, 211–221. https://doi.org/10.1006/jmbi.1999.2761.
[61] Zatyka, M., Bingle, L., Jones, A.C., Thomas, C.M., 2001. Cooperativity between *KorB* and *TrbA* repressors of broad-host-range plasmid RK2. J Bacteriol 183, 1022–1031. https://doi.org/10.1128/jb.183.3.1022-1031.2001.
[62] Zatyka, M., Jagura-Burdzy, G., Thomas, C.M., 1997. Transcriptional and translational control of the genes for the mating pair formation apparatus of promiscuous IncP plasmids. J Bacteriol 179, 7201–7209. https://doi.org/10.1128/jb.179.23.7201-7209.1997.
[63] Dabrzalska, M., Janaszewska, A., Zablocka, M., Mignani, S., Majoral, J.P., Klajnert-Maculewicz, B., 2017. Cationic phosphorus dendrimer enhances photodynamic activity of Rose Bengal against basal cell carcinoma cell lines. Mol Pharm 14, 1821–1830. https://doi.org/10.1021/acs.molpharmaceut.7b00108.
[64] Nakonechny, F., Barel, M., David, A., Koretz, S., Litvak, B., Ragozin, E., et al., 2019. Dark antibacterial activity of Rose Bengal. Int J Mol Sci 20. https://doi.org/10.3390/ijms20133196.
[65] Ilizirov, Y., Formanovsky, A., Mikhura, I., Paitan, Y., Nakonechny, F., Nisnevitch, M., 2018. Effect of photodynamic antibacterial chemotherapy combined with antibiotics on Gram-positive and Gram-negative bacteria. Molecules 23. https://doi.org/10.3390/molecules23123152.
[66] Wang, Y., Xu, Y.X., Guo, X.H., Wang, L., Zeng, J., Qiu, H.X., et al., 2022. Enhanced antimicrobial activity through the combination of antimicrobial photodynamic therapy and low-frequency ultrasonic irradiation. Adv Drug Deliv Rev 183. https://doi.org/10.1016/j.addr.2022.114168.
[67] Hao, Y., Chung, C.K., Yu, Z.F., t Veld, R., Ossendorp, F.A., ten Dijke, P., et al., 2022. Combinatorial therapeutic approaches with nanomaterial-based photodynamic cancer therapy. Pharmaceutics 14. https://doi.org/10.3390/pharmaceutics14010120.
[68] Perez-Laguna, V., Barrena-Lopez, Y., Gilaberte, Y., Rezusta, A., 2021. *In vitro* effect of photodynamic therapy with different lights and combined or uncombined with chlorhexidine on *Candida* spp. Pharmaceutics 13. https://doi.org/10.3390/pharmaceutics13081176.
[69] Guo, Y.Y., Rogelj, S., Zhang, P., 2010. Rose Bengal-decorated silica nanoparticles as photosensitizers for inactivation of Gram-positive bacteria. Nanotechnology 21. https://doi.org/10.1088/0957-4484/21/6/065102.
[70] Elkihel, A., Vernisse, C., Ouk, T.S., Lucas-Roper, R., Chaleix, V., Sol, V., 2023. Xylan-porphyrin hydrogels as light-triggered Gram-positive antibacterial agents. Gels 9. https://doi.org/10.3390/gels9020124.
[71] George, S., Hamblin, M.R., Kishen, A., 2009. Uptake pathways of anionic and cationic photosensitizers into bacteria. Photochem Photobiol Sci 8, 788–795. https://doi.org/10.1039/b809624d.
[72] Nagata, J.Y., Hioka, N., Kimura, E., Batistela, V.R., Terada, R.S.S., Graciano, A.X., et al., 2012. Antibacterial photodynamic therapy for dental caries: evaluation of the photosensitizers used and light source properties. Photo Photodyn Ther 9, 122–131. https://doi.org/10.1016/j.pdpdt.2011.11.006.